ELSEVIER

PII: S0309-1708(98)00041-4

Advances in Water Resources Vol. 22, No. 6, pp 633–644, 1999

0309-1708/99/$ – see front matter

Evaluation of pore water pressure fluctuation around an advancing longwall face

J. Liu[a,*] & D. Elsworth[b]

[a]*Department of Civil Engineering, The University of Western Australia, Nedlands, Perth 6907, Australia*
[b]*Department of Mineral Engineering, The Pennsylvania State University, University Park, PA 16802, USA*

(Received 18 May 1997; revised 6 July 1998; accepted 28 July 1998)

Large deformations that accompany longwall mining result in complex spatial and temporal distributions of changes in undrained pore fluid pressures around the advancing face. These seemingly anomalous changes are recorded in the rapid water level response of undermined and adjacent wells, and may be explained in the short-term as a undrained poroelastic effect. A three-dimensional finite element model is applied to define anticipated pore fluid response both around the advancing mining face, at depth, and in the near surface region. The results are carefully verified against the response recorded at three well-instrumented longwall sites. Pore pressure changes are indexed directly to volumetric strains defining zones of significant depressurization in the caving zone and in zones of extension adjacent to the subsidence trough on the ground surface. Overpressurization occurs in the abutment region, at panel depth, and in the surface compressive zone immediately inside the angle-of-draw. These results are confirmed with available, short-term water level response data, defining the strongly heterogeneous spatial response and the significance of well depth on anticipated water level response.

1 INTRODUCTION

Underground mining by *full extraction* methods, such as longwall mining, is becoming increasingly popular for mining uninterrupted and near horizontal seams. Longwall mining involves extracting coal in large blocks, called panels, using a mechanized shearer. The full seam thickness, of perhaps 1–2 m, is removed and panel extents are typically 200–350 m wide and up to 3000 m in length. Multiple panels comprise a single mining operation. With this method, the mine roof is supported with hydraulic supports that automatically advance as mining progresses. As the supports move, the mine roof is allowed to collapse into the mine void. Strata above the mine level are altered as the mine roof caves behind the shields (hydraulic supports), creating zones where blocks of rock fill the mine void, or fracture or deform as rock layers warp downward. These alterations in overburden characteristics potentially induce large strains in the overlying strata that in turn result in a strongly heterogeneous and anisotropic hydraulic conductivity field[1–5] and simultaneously inducing large "undrained" changes in pore fluid pressures. These undrained changes are recorded as raised or depressed water levels in the zone immediately surrounding the advancing face[6,7]. Despite the acknowledgment that mining-induced strains may be substantial, no comprehensive description of this behavior has been advanced. Some results for two-dimensional geometries have been reported[8,9] but these neglect the true three-dimensional complexity of the zone immediately surrounding the advancing face. This behavior is examined in the following.

Undermined strata typically have a complicated internal structure and stress state, both of which are, in large part, unknown and perhaps unknowable. This would appear to make solution for the mining-induced, strain field intractable. However, some alternatives may be pursued to avoid using parameters

*Corresponding author. Current address: Environmental Engineering Group, CSIRO Exploration & Mining, Private Bag, PO Wembley, WA 6014, Australia. E-mail: jliu@per.dem.csiro.au; tel: 61-8-9333-6189; fax: 61-8-9387-8642

that are unlikely available in practice. The subsidence field that develops around a longwall panel is, surprisingly, relatively insensitive to the material properties of deformation modulus and strength due to the displacement controlled nature of the process[10,11,19]. Therefore, the mining-induced strain field, defined by the subsidence profile, may also be decoupled from the material parameters describing the overlying strata. Once the strain field is defined as unique for any given mining geometry, fluctuations in pore water pressure around the longwall face can be evaluated provided a link between mining-induced strain and change in pore water pressure is established. This is the underlying scientific rationale of the work reported here.

2 EVALUATION OF MINING-INDUCED STRAIN FIELD

The subsidence field that develops around a longwall panel can be determined directly from empirical observations[12]. These data relate the subsidence and strain profiles to parameters describing, mining depth, h_m, mining width, w, and seam thickness, t, alone, as illustrated in Fig. 1. The relative insensitivity of the resulting subsidence profile to the material properties of deformation modulus and strength results from the overriding influence of geometric controls on deformation. Following mining, the panel span is typically sufficiently large that closure between panel floor and roof is unavoidable. Consequently, the resulting strain field, $\Delta\underline{\varepsilon}$ (strain vector incurred by mining), is uniquely defined in terms of the parameters[10]

$$\Delta\underline{\varepsilon} \approx f\left[\frac{w}{t}, \frac{w}{h_m}\right] \tag{1}$$

where the influence of topography is also included in the ratio of width to mining depth, w/h_m. Consequently, the strain field may be uniquely defined given that these geometric parameters are known, a priori, and the analysis is now completely decoupled from the material parameters describing the overburden strata. This lack of sensitivity has important considerations in reducing to a minimum the data required to complete an appraisal of the subsidence effect. This displacement controlled nature of subsidence allows simplification of the actual fractured rock mass as an equivalent continuous deformation model.

2.1 Finite element representation

It is assumed that the rock mass is isotropic but heterogeneous. The resulting finite element formulation for the solid phase is symbolically defined as

$$\underline{K}_s\, \underline{d} = \underline{f} \tag{2}$$

where $\underline{K}_s$ is the stiffness matrix of the solid phase, $\underline{d}$ is the nodal displacement vector, and $\underline{f}$ is the nodal force vector. The stiffness matrix, $\underline{K}_s$, in eqn (2) is defined as

$$\underline{K}_s = \int\int_v\int \underline{B}^T\, \underline{D}\, \underline{B}\, dx\, dy\, dz \tag{3}$$

where $\underline{B}$ is a geometric matrix, $\underline{D}$ is material properties matrix and a function of the elastic modulus, E, and the

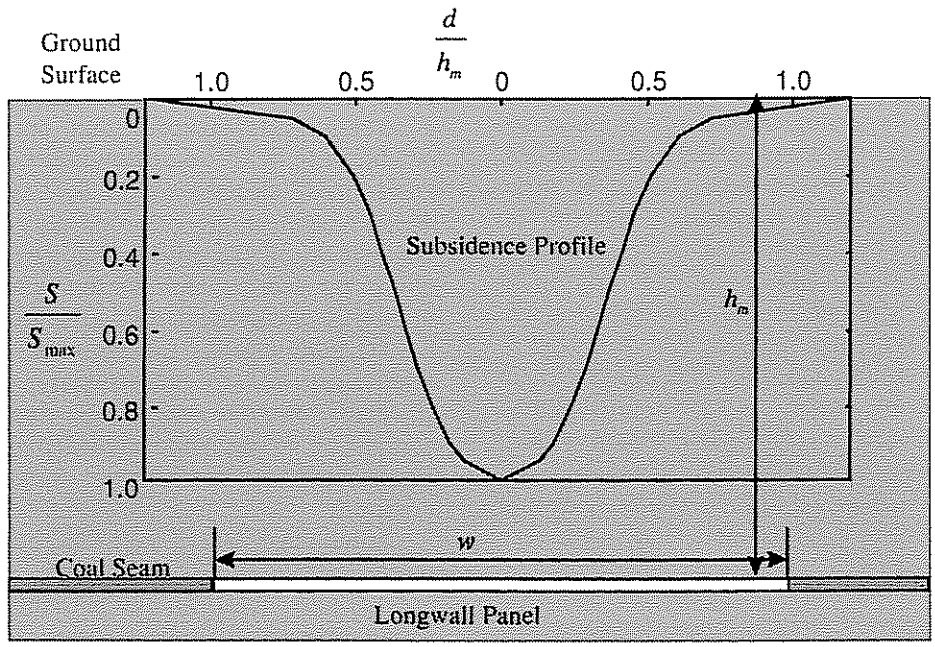

Fig. 1. Predicted subsidence profile based on the mining geometry. Where d is the horizontal distance from the panel center, S is the subsidence at the distance d, and S_{max} is the maximum subsidence. It is assumed in the example that w/h_m is equal to 1.

Poisson ratio, μ, and v is the volume. The mining-induced strain vector can be obtained as

$$\Delta\underline{\varepsilon} = \underline{B}\ \underline{d} \tag{4}$$

Based on the mining-induced strain vector, $\Delta\underline{\varepsilon}$, the volumetric strain for each element is obtained as

$$\Delta\varepsilon_v = \Delta\varepsilon_x + \Delta\varepsilon_y + \Delta\varepsilon_z \tag{5}$$

where $\Delta\varepsilon_x$, $\Delta\varepsilon_y$, and $\Delta\varepsilon_z$ are mining-induced strains in the x-, y- and z-directions, respectively.

The displacement controlled nature of subsidence is implemented in the finite element model (FEM) through two different nonlinear material models representing the overburden failure and the coal extraction, respectively. These two nonlinear material models are presented in the following.

2.2 Representation of overburden failure

Notice that the $\underline{B}$ matrix in eqn (3) remains fixed during the solution procedure, and only the $\underline{D}$ matrix has to be adapted at each iteration. This is achieved at the end of each iteration by calculating the maximum principal stress, σ_{11}, and modifying the "effective" elastic parameters as

$$E = \begin{cases} E_0 & \sigma_{11} < 0 \\ \frac{E_0}{R_e} & \sigma_{11} \geqslant 0 \end{cases} \tag{6}$$

$$\mu = \begin{cases} \mu_1 & \sigma_{11} < 0 \\ \mu_2 & \sigma_{11} \geqslant 0 \end{cases} \tag{7}$$

where E is elastic modulus of the overburden, E_0 is elastic modulus of elements in compression, E_0/R_e is elastic modulus of elements in extension, μ_1 is Poisson ratio of elements in compression, μ_2 is Poisson ratio of elements in extension, and σ_{11} is the maximum principal stress. The magnitude of R_e is obtained by matching the "field-measured" or estimated maximum subsidence.

2.3 Representation of coal extraction

A similar nonlinear modulus model is used to represent the process of coal extraction. The main advantage of this method is that elements do not have to be removed from the mesh in order to simulate coal extraction, and excavation boundary tractions do not need to be calculated. More importantly, the prescribed displacement boundary conditions around the longwall panel can be successfully implemented. The $\underline{D}$ matrix, as shown in eqn (3), for in-panel elements has to be adapted at each iteration. This is achieved at the end of each iteration by calculating the vertical strain ε_z

$$E_p = \begin{cases} E_{p0} & \varepsilon_z > -1.0 \\ 10^n E_{p0} & \varepsilon_z \leqslant -1.0 \end{cases} \tag{8}$$

where E_p is modulus of the material comprising the panel, E_{p0} is initial modulus of the panel material (before mining) and ε_z is vertical strain within the panel material. This simple model prevents the interpenetration of the panel roof and floor by changing the panel modulus at contact, where n may be assigned any reasonable large numbers.

2.4 Evaluation of pore water pressure fluctuation

The constitutive equations that extend standard linear elasticity to poroelastic materials are expressed as[13–15]

$$\varepsilon_{ij} = \frac{\sigma_{ij}}{2G} - \left(\frac{1}{6G} - \frac{1}{9K}\right)\delta_{ij}\sigma_{kk} + \frac{1}{3H}\delta_{ij}p \tag{9}$$

$$\theta = \frac{\sigma_{kk}}{3H} + \frac{p}{R} \tag{10}$$

where ε_{ij} is the strain tensor, σ_{ij} is the stress tensor, θ is the fluid content, and δ_{ij} is the Kronecker delta function. In the absence of the pore pressure, p, eqn (9) degenerates to the classic elastic relation. Parameters, K and G, are identified as the bulk and the shear modulus of the drained elastic solid. Additional constitutive constants, H and R, characterize the coupling between the solid and fluid stress and strain.

The constitutive equations of an isotropic poroelastic material can actually be separated into a deviatoric response

$$e_{ij} = \frac{1}{2G}s_{ij} \tag{11}$$

and a volumetric one

$$\Delta\varepsilon_v = -\left(\frac{P}{K} - \frac{p}{H}\right) \tag{12}$$

$$\theta = -\left(\frac{P}{K} - \frac{p}{R}\right) \tag{13}$$

where e_{ij} and s_{ij} denote the deviatoric strain and stress, P the mean or the total pressure (isotropic compressive stress), ε_v the volumetric strain, and θ is variation of fluid content per unit volume of porous media. Strains are defined positive in extension and increases in fluid pressure are defined positive. Under completely undrained conditions, the change in fluid content is null ($\theta = 0$), and eqn (13) becomes

$$p = \frac{R}{K}P = B_s P \tag{14}$$

where B_s is known as the Skempton pore pressure coefficient[15]. Substituting eqn (14) into 12 yields

$$p = -Q\Delta\varepsilon_v \tag{15}$$

where

$$Q = -\left(\frac{1}{B_s K} - \frac{1}{H}\right)^{-1} \tag{16}$$

and $\Delta\varepsilon_v$ is obtained through eqn (5). It is shown in eqn (16) that change in pore water pressure is proportional to mining-induced volumetric strain. Compressive

volumetric strain results in a rise of pore water pressure, and extensional volumetric strain results in a fall of pore water pressure. Equation 15 is used to evaluate the distribution of post-mining overburden depressurization zones in the following sections.

3 RESULTANT FE FORMULATION AND SOLUTION PROCEDURE

As a summary, the resultant finite element representation for the evaluation of the pore water pressure fluctuation around an advancing longwall face is formulated as

$$\underline{K}_s(d)\underline{d} = \underline{f} \tag{17}$$

$$\Delta\underline{\varepsilon} = \underline{B}\ \underline{d} \tag{18}$$

Solution for the mining-induced strains is directly used to evaluate the volumetric strain, $\Delta\underline{\varepsilon}$, and the consequent change in pore water pressure for each element, as defined in the following

$$\Delta\varepsilon_v = \Delta\varepsilon_x + \Delta\varepsilon_y + \Delta\varepsilon_z \tag{19}$$

$$p = -Q\Delta\varepsilon_v. \tag{20}$$

The pore water pressure fluctuations around an advancing longwall mining face are evaluated through the following straightforward steps: (1) The strain field that develops around a longwall panel as a result of mining is obtained through solving eqns (17) and (18), using a nonlinear FE model that accommodates the influence of material failure and self-weight; (2) From this predicted strain field, the volumetric strain for each element is obtained through solving eqn (19); and (3) With the mining-induced volumetric strains determined, the change in pore water pressure is obtained through solving eqn (20). The validation of the resultant FE model is well documented in studies[11,16–19]. The following documents the application of this FE model to a well instrumented longwall mine site as a three-dimensional example. Through this application, the complex three-dimensional hydraulic responses of overburden to longwall mining around the advancing mining face are thoroughly examined. These results are reported in the following sections.

4 APPLICATION

An extensive hydrological and geomechanical monitoring program was conducted at a longwall coal mine in West Virginia[7]. Ground water levels, pre-mining hydraulic conductivity, overburden movement, and surface subsidence relative to the passage of the longwall panel were obtained through this monitoring program. Based on this information, the mining-induced overburden strain field and the change in pore water pressure around the longwall face are evaluated under constrained drainage conditions. Results of the evaluation are verified against the in situ monitoring results.

4.1 Site specification and field monitoring

The mine is located within the Pittsburgh seam, with an average extraction thickness at the study site ranging from 1.7 to 1.8 m (5.5 to 6 feet). The instrumented panel is 183 m (600 feet) wide by 2195 m (7200 feet) long. The overburden monitoring test site is located at approximately center-panel length. The test site lies ontop of a broad crest at the end of a long steep-side ridge. Relief to the stream valley below is 91 to 122 m (300 to 400 feet). The coal seam is approximately 213 to 219 m (700 to 720 feet) deep at the test site. The mined seam lies directly beneath about 85 m (280 feet) of highly competent limestone and sandstone strata as contrasted with the low strength shales and claystones close to the surface.

The shallow water-bearing strata at the test location are considered to be perched or semiperched aquifers, which consist of a vertical succession of water tables separated by unsaturated zones. Low permeability shales and claystones impede the downward migration of ground water, and water levels decrease as well depth increases. Aquifer recharge is almost entirely from precipitation in the form of snow and rain, and discharge occurs via springs, seeps along hillsides and via evapotranspiration. Pre-mining water levels in wells drilled within the upper 60 m (200 feet) fluctuate widely with seasonal changes in precipitation patterns and evapotranspiration. Steep topography is known to have played an important role in shallow aquifer water level fluctuation, since the high runoff and small recharge area greatly limit recharge. Pre-mining water levels below 122 m (400 feet) remained fairly constant.

Ground water monitoring was conducted in a total of eight monitoring wells and one private well. Six of the monitoring wells and the private well were located near the panel-center. Three of those wells (W1, W3 and W5) were completed to a depth of 183 m (600 feet). Of the two wells drilled over the panel headgate, well W7 was completed to a depth of 123 m (405 feet). The other four wells W2, W4, W6 and the private well were completed to a depth of less than 62 m (200 feet).

4.2 Field ground water monitoring results

Hydraulic responses were observed through eight monitoring wells. In general, water levels in shallow wells [W2, W4 and W6, less than 62 m (200 feet) deep] and

near center-panel were lowered (or went dry) within one month of being undermined, then recovered to near pre-mining levels, four to five months after mining. Sustained post-mining water levels in these shallow wells exhibited less fluctuation and were slightly lower than average pre-mining levels. The 183-m (600-foot) deep wells (W1, W3, and W5) went dry after the face had passed 15 m (50 feet) and did not recover. The 123-m (405-foot) well (W7) over the headgate was relatively unaffected in the long term by passage of the face.

4.3 Three-dimensional numerical model

In the following analysis, both the deformation analysis and the hydraulic response are assumed under steady state conditions, although this process is necessarily iterative, since effective stresses depend on pore pressure magnitudes. However, the effects of changes in pore fluid pressures are overwhelmed by changes in total stresses, and strains may be adequately estimated without consideration of pore fluid effects. This is the case, for example in the consideration of permeability changes occasioned from longwall mining, verified in previous studies[8,9,20]. The evaluation of fully coupled (poroelastic) systems involving single[8] and dual[9] porosity behavior has confirmed the short-lived nature of the transient poroelastic effects. Similarly, analyses with steady-state coupling for effective stresses[20] have indicated the trivial contribution of effective stresses over the massive realignment of total stresses conditioned by mining. This assumption is not a requirement of this analysis, as strain distributions may be evaluated, inclusive of effective stress effects. However, this decoupling greatly simplifies the ensuing analysis, with little loss of applicability.

The three-dimensional FE model, developed for both the determination of overburden deformation and post-mining hydrologic effects is illustrated in Fig. 2. Boundary mesh deformations in the x-direction at the cross sections of $X = 0$ and $X = 1000$ m, in the y-direction at the cross sections of $Y = 0$ and $Y = 600$ m, and in the z-direction at the bottom ($Z = 0$) are constrained for the determination of overburden deformation. No-flow boundary conditions are applied at the cross sections of $X = 0$ and $Y = 0$, and constant head boundary conditions are applied ($h = 400$ m) at the cross sections of $X = 1000$ m and $Y = 600$ m and around the panel ($h = 188.2$ m for the floor, $h = 190$ m for the roof). This enables the post-mining ground water regime to be determined, with the inclusion of deformational effects. The values of the modulus of elasticity for the overburden are assumed as $E = 4 \times 10^9$ Pa and 0.30, respectively. The post-failure values of the Poisson ratio and elastic modulus in extensional elements, are obtained as 0.45 and $E/4$, respectively, by matching the maximum model subsidence with the field-measured one.

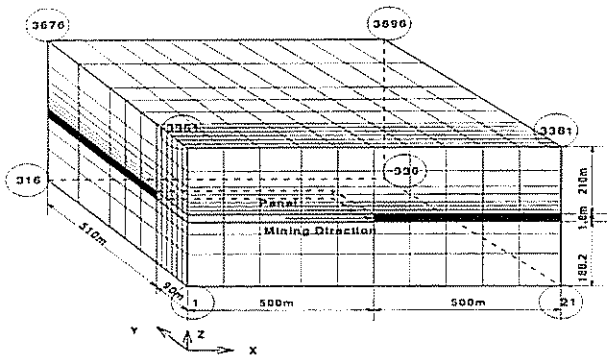

Fig. 2. FE models for both the determination of overburden deformation and the post-mining hydrologic regime. Circled numbers are nodal numbers. Model used quarter symmetry of the panel, centered on the origin. Panel depth is 210 m below surface. Solid black represents un-mined coal.

4.4 Distribution of mining-induced strains

The modeled subsidence cone is illustrated in Fig. 3(a) and the final subsidence profile at the cross section of $X = 0$ is compared with field data in Fig. 3(b). It is apparent that the model subsidence profile is flatter than the field measured one. This may be due to a number of factors such as the possible discontinuous deformation of overburden, the deviation of basic

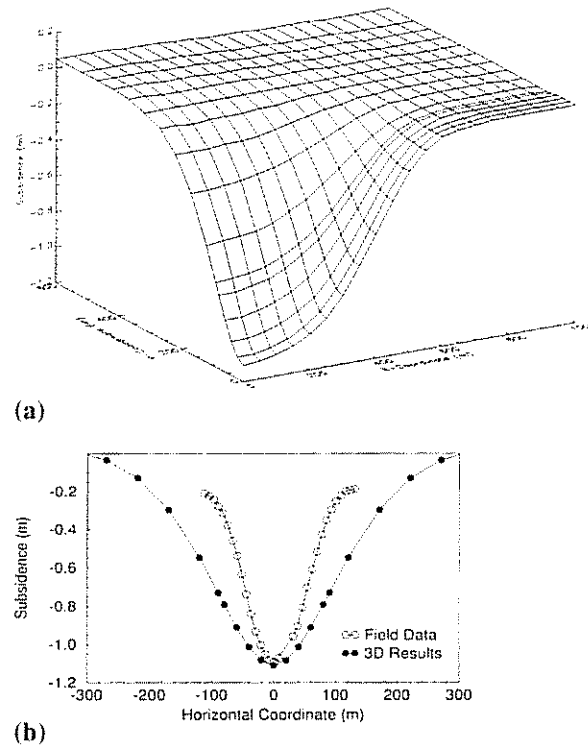

Fig. 3. Subsidence due to longwall mining. (a) Subsidence cone. (b) Comparison of model data with field data in the cross section of $X = 0$.

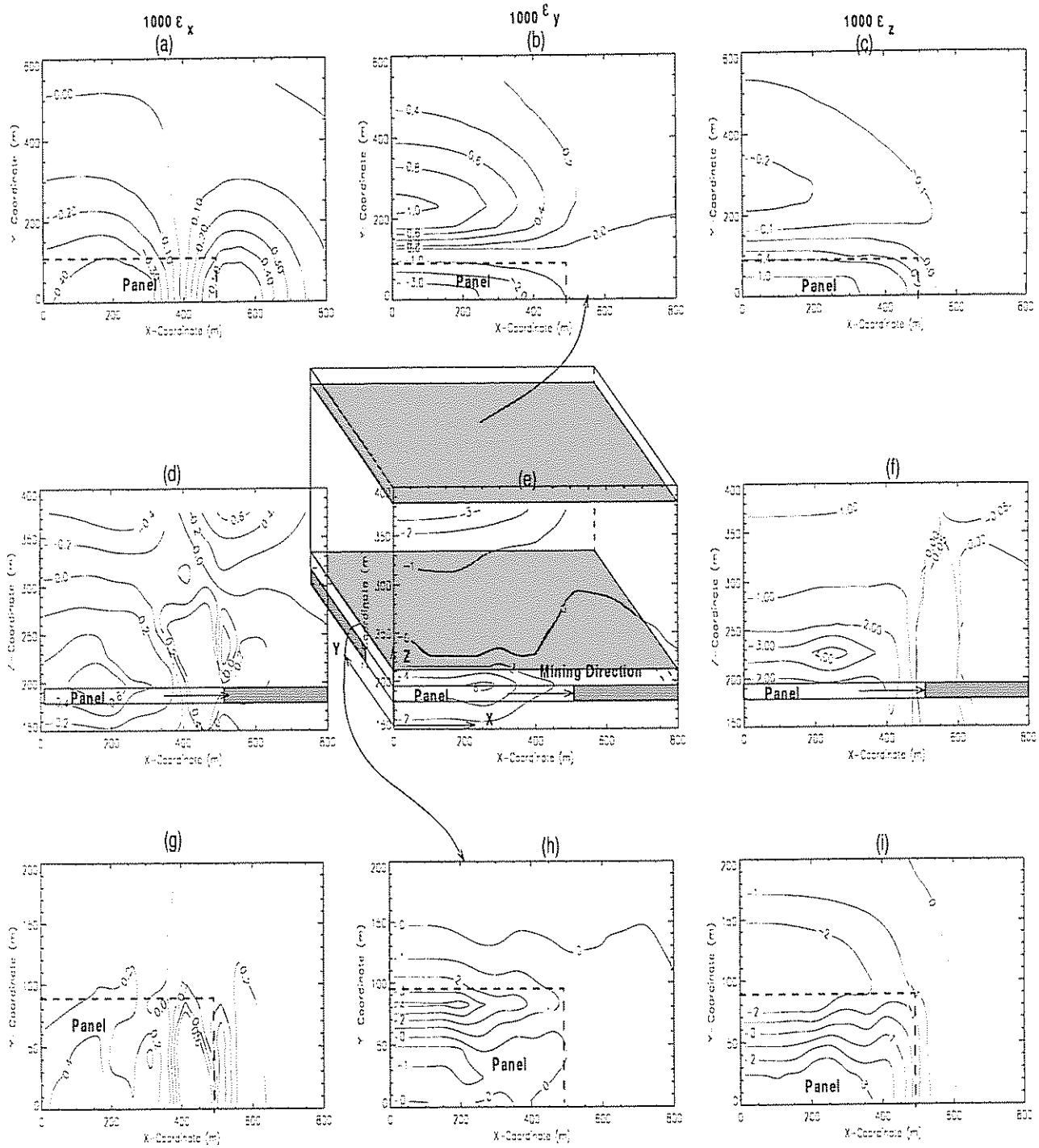

Fig. 4. Contours of normalized strains at different cross sections. (a), (b) and (c) represent strains in a horizontal plane in the near surface zone. (d), (e) and (f) represent strains in a vertical section along the panel centerline. (g), (h) and (i) represent strains in a horizontal plane immediately above the panel roof. Figures in the columns represent normal strains in the global x-, y- and z-directions, respectively.

assumptions from reality, and the possible numerical errors. Nevertheless, the mismatch between the measured and modeled subsidence profiles may be considered adequate for the subsequent analyses. The strain field, modulated by the surface subsidence profile, is illustrated in Fig. 4. Apparent from these figures is that significant mining-induced overburden extensional deformation is restricted to shallow depths (less than 100 m deep) ahead of the advancing face, but more significant mining-induced extensional deformation develops behind the advancing face, particularly in the caving zone and in shear zones above

the abutments. These include the typically acknowledged failure zones enclosed within the envelope of the angle-of-draw, and the complex zone of rapidly changing strains, characterizing the intersection of the angle of draw with the ground surface. The evaluated strain field enables undrained changes in pore fluid pressures, recorded as water level rises or depressions in wells, to be evaluated.

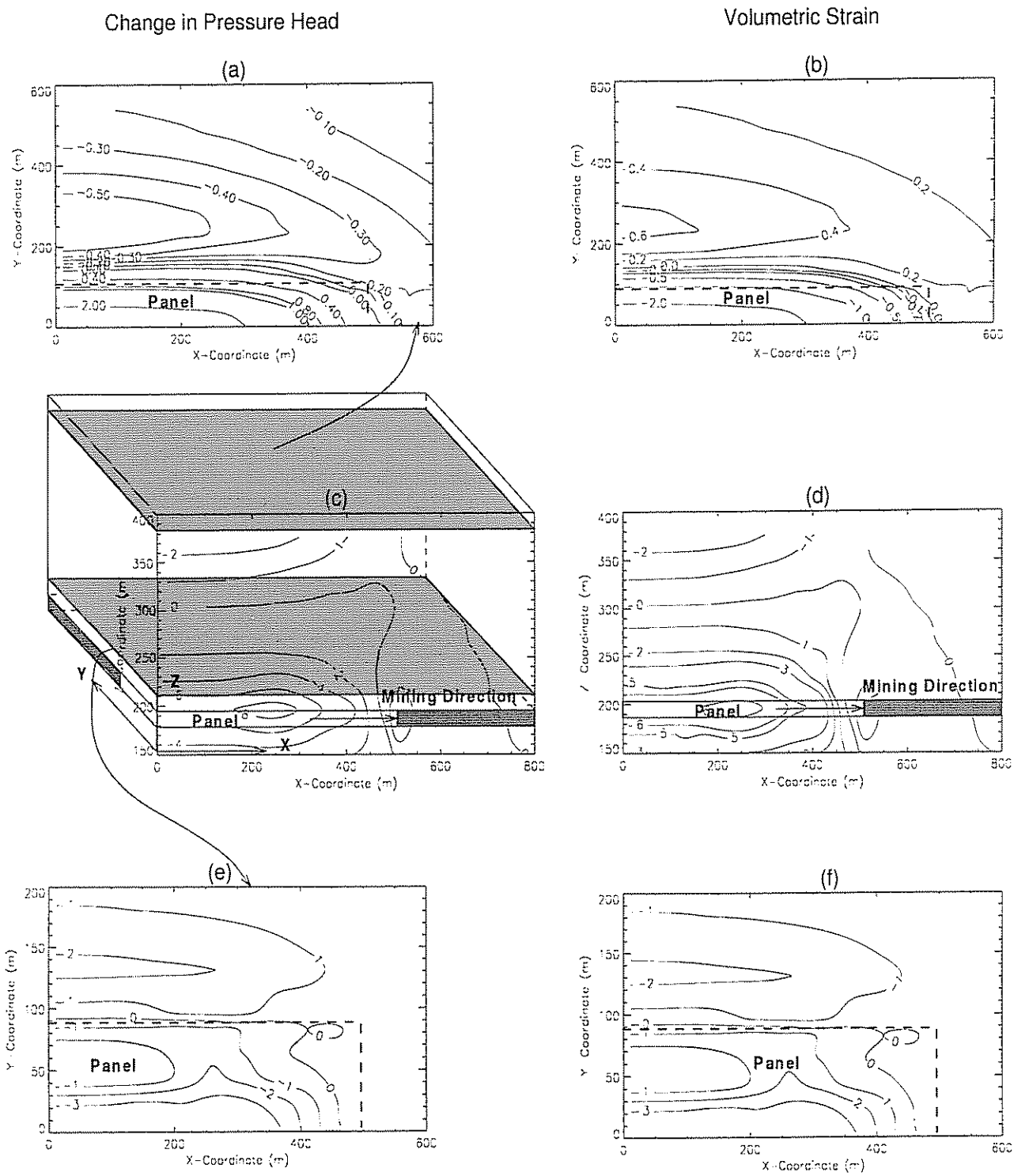

Fig. 5. Diffusion–deformation coupling effects during longwall mining at different cross sections. (a) and (b) represent changes in dimensionless pressure head and volumetric strains in a horizontal plane in the near surface zone. (c) and (d) represent changes in dimensionless pressure head and volumetric strains in a vertical section along the panel centerline. (e) and (f) represent changes in dimensionless pressure head and volumetric strains in a horizontal plane immediately above the panel roof. Negative values represent decrease in pressure and compressive strain.

4.5 Determination of overburden depressurization

Equation 15 can be written as

$$\frac{\Delta h}{Q} = -\Delta \varepsilon_v \tag{21}$$

where Δh is the change in pressure head due to longwall mining under completely undrained conditions, and $\Delta \varepsilon_v$ is the mining-induced volumetric strain. The numerical results of normalized volumetric strains and changes in dimensionless pressure ($\Delta h/Q$) due to longwall mining for different cross sections are illustrated in Fig. 5.

As illustrated in Fig. 5(a), the dimensionless pressure head inside the confines of the panel (but above the panel) and within the shallow aquifer declines within about 200 m ahead of the working face, significantly rises behind the working face, and declines in the zone beyond the panel but within the angle of draw. Therefore, the zones of depressurization are outside the mining panel and the zone of pressurization is within the panel in the near surface. As illustrated in Fig. 5(c), more significant changes in dimensionless pressure head develop behind the advancing face, particularly in the caving zone (depressurization) and at the ground surface (pressurization). Therefore, the zone of slight change in dimensionless pressure head is restricted to the deep reaches of the section (right above the coal seam) ahead of the advancing face at the longitudinal cross section. As illustrated in Fig. 5(e), the dimensionless pressure head inside the confines of the panel and within the deep aquifer rises within about 100 m ahead of the working face, significantly declines behind the working face, and rises in the zone beyond the panel but within the angle of draw. Therefore, in generality, the zones of pressurization are outside the mining panel and the zone of depressurization is within the panel at the cross section (directly above the coal seam).

Changes in dimensionless pressure head distribution with depth at different cross sections are illustrated in Fig. 6. Apparent from Fig. 6(a) is that the hydraulic response of the surface zone (represented by unfilled circles) is very different from that of the immediate zone (represented by filled circles). In the shallow aquifer, the zone of pressurization is essentially confined within the panel area and the zones of depressurization are beyond the panel confines. For the deep immediate zone, the region of depressurization is within the panel area and the regions of pressurization are external to this. In the longitudinal section, the hydraulic response of the surface zone is also very different from that of the immediate zone, apparent from Fig. 6(b). The zone of pressurization in the surface zone is within the panel area, however, at depth the zone above the panel is depressurized with pressurization apparent ahead of the working face.

Based on these results as shown in Figs. 5 and 6, it is concluded that: (1) The piezometric level in a shallow well located within the vertical confines of the panel first declines as the working face approaches and then

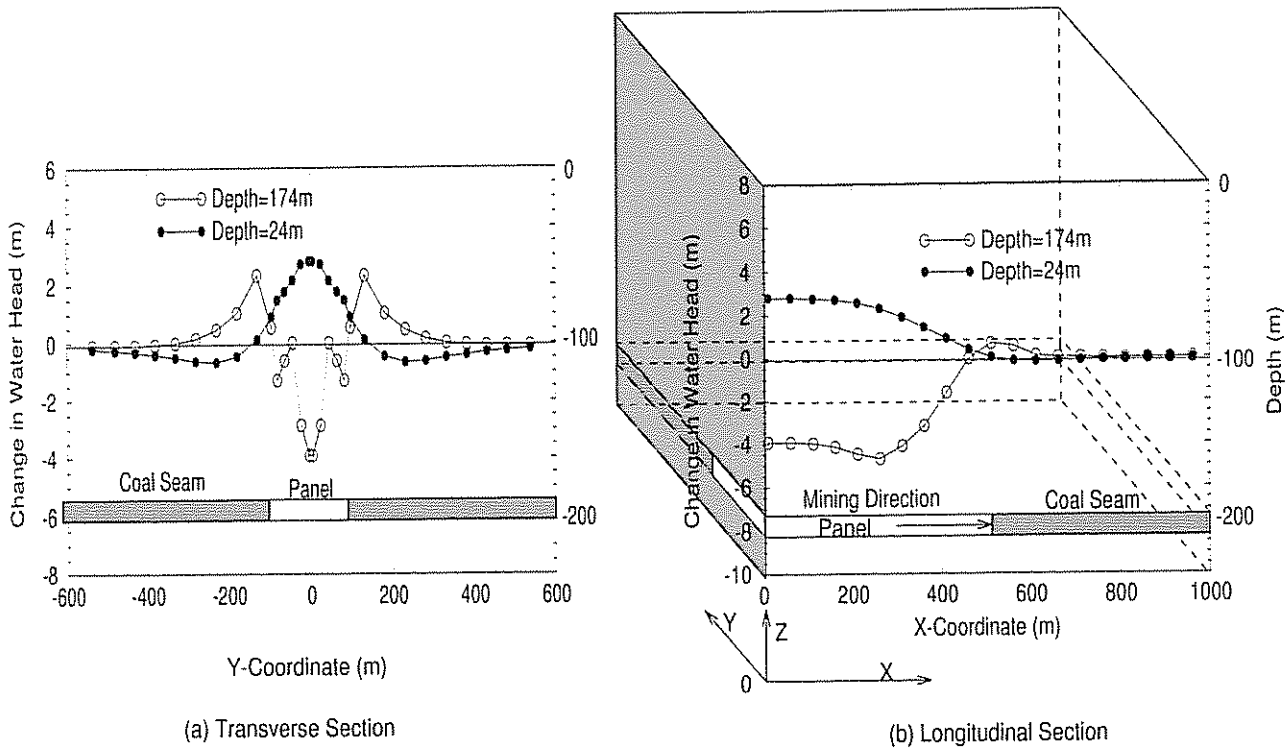

Fig. 6. Changes in dimensionless pressure head ($1000(\Delta h/Q)$) due to longwall mining for transverse (a) and longitudinal (b) vertical sections centered on the panel.

significantly rises after the working face passes the well; (2) The piezometric level in a shallow well located outside the panel, but within the angle of draw, declines first as the working face approaches and continues to decline after the working face passes the well; (3) The piezometric level in a deep well located within the panel first rises as the working face approaches and then significantly declines after the working face passes the well; (4) The piezometric level in a deep well located outside the panel, but within the angle of draw, rises as the working face approaches and continues to rise after the working face passes the well; (5) Wells positioned at the centerline of a longwall panel exhibit the greatest fluctuations (head loss in the immediate zone and head gain in the surface zone), as shown in Fig. 5(a), (e) and 6. The fluctuation of water levels in a shallow well occurs when the advancing

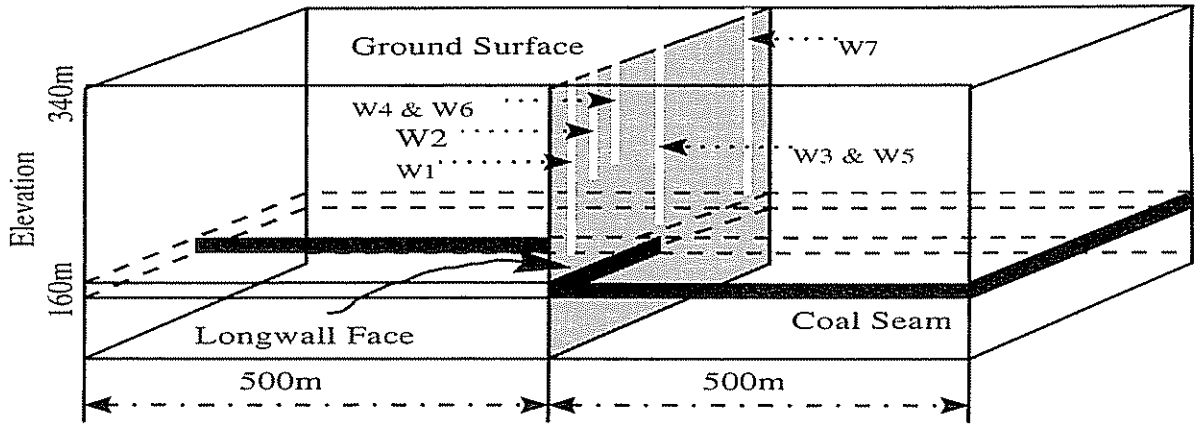

(1)

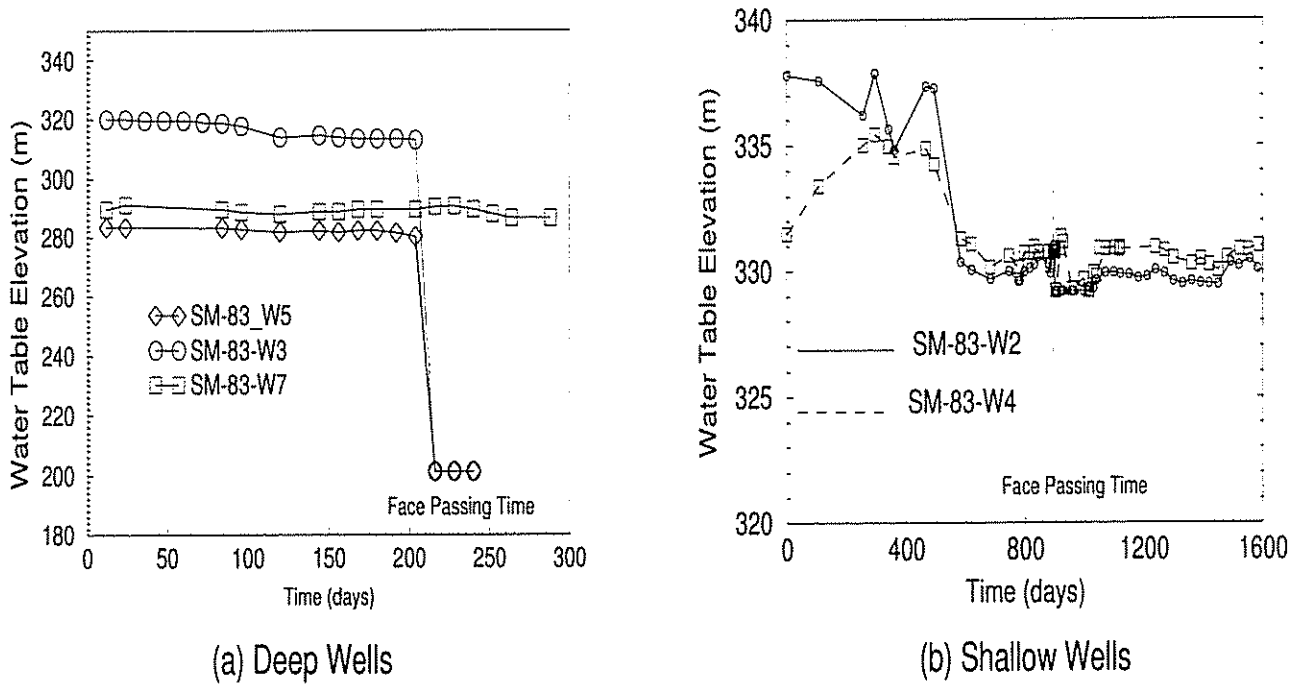

(2)

Fig. 7. Observed fluctuation of water levels in monitoring wells. (1) Monitoring well locations with completion intervals relative to the geometry of the transverse section. (2) Observed water level records of monitoring wells during undermining relative to the time of advancing face passage.

face is approximately one thickness of the overburden ahead of the well (as shown in Fig. 5(a)). This is consistent with observed results[7], as shown in Fig. 7.

These conclusions must be modified when drainage conditions are taken into consideration and the assumption of "undrained" loading is violated. Fluctuation of piezometric levels in water wells is a function of the well location relative to the mine layout, the proximity of mining and wellbore storage characteristics. This confirms that wells are generally unaffected by mining of a preceding panel unless they are located within the angle of draw[6]. The validity of this statement may be examined by directly using superposition of the strain fields illustrated previously. Correspondingly, conclusions drawn from the single panel case may be directly applied to multi-panel cases.

These conclusions are also verified by both specific and anecdotal evidence available from a number of studies[6,16,2,21]. A typical observed fluctuation[6] for a shallow well during the process of mining is illustrated in Fig. 8. For this example, the study area overlies four adjacent longwall panels spaced on 300 m centers and approximately 190 m wide and 2500 m long. The mining occurs in the Pittsburgh Coalbed, which is typically 1.8 to 2 m thick in the study area with an overburden thickness ranging from 210 to 300 m. Well No.4 is about 50 m deep and on the panel centerline. As shown in Fig. 8, the rate of decline in water level decreases as the dynamic development of strain changes from extension to compression. The rate of recovery is the greatest when the overburden is subject to maximum compressive strain. In this well only the extensional strain significantly affected the fluid levels. The compressive phase of the derived strain curve did not appear to significantly control either the rise or decline of the fluid level, possibly due to the development of fracturing and the deviation from true "undrained" conditions, or more likely due to the stiffer behavior of the rock mass in compression. These observed results are consistent with the model results.

The previous conclusions, concerning the fluctuation of water levels within deep wells located within panel

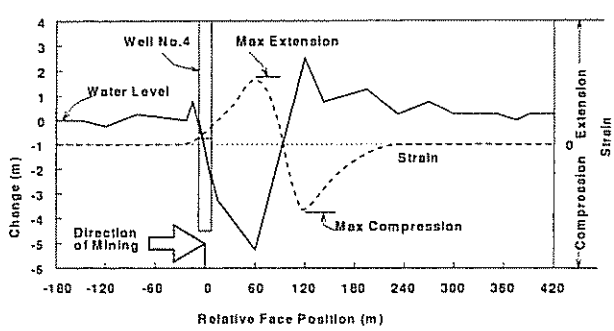

Fig. 8. Rate of water level fluctuation and strain as a function of relative face position for Well No.4 (50 m deep and at the panel centerline).

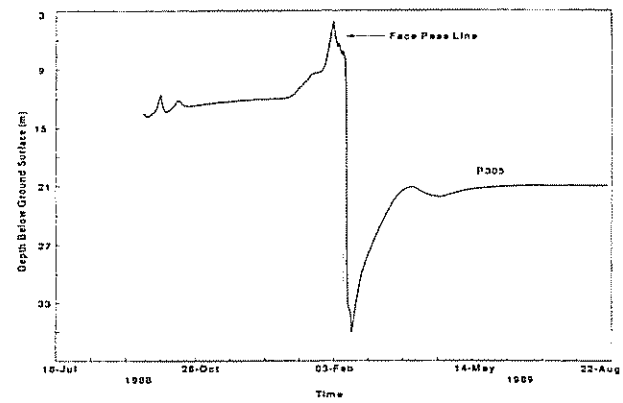

Fig. 9. Fluctuation of piezometric levels for the piezometer P305 due to longwall mining.

boundaries, is further verified[2]. This longwall mine was operated at about 221 m depth in a 3 m thick seam. The 18 m thick aquifer is located at a depth of about 24–27 m, overlain by a shale aquitard. The longwall panels are 180 m wide, about 1500 m long and separated by a 60 m spacing with double barrier pillars. The fluctuation of water levels in piezometer P305 (100 m deep piezometer completed in shale at the panel centerline) is illustrated in Fig. 9. The piezometric level rose rapidly by about 8 m immediately before the subsidence wave reached the location and then fell dramatically (49 m in one day) at the onset of subsidence.

The conclusions drawn with respect to shallow wells located both within the panel and outside the panel, but within the angle of draw, are verified by another case study[21]. The longwall mine is located in the gently rolling farmland of southeastern Illinois, and produces from a 2 m thick coal seam at a depth of 120 m. A 3 to 5 m thick sandstone aquifer is present at a depth of 56 m beneath the 203 m wide by 2400 m long panel. The fluctuation of water levels in two piezometers TP2 (located at the panel centerline) and TP3 (located within the maximum extensional zone at the panel side) are illustrated in Fig. 10. The water level in TP2

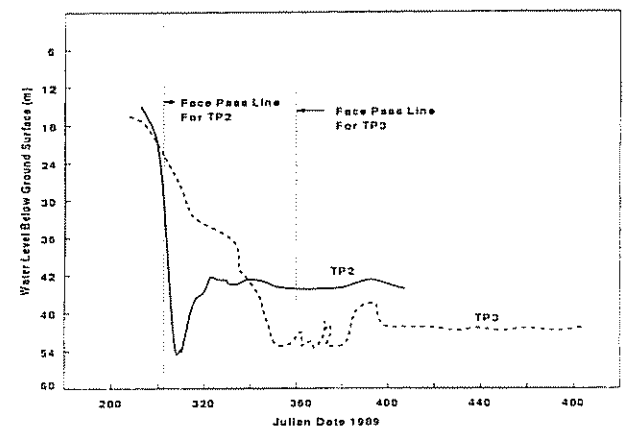

Fig. 10. Fluctuation of piezometric levels for Trivoli piezometers TP2 and TP3 due to longwall mining.

first rose and then declined as the active face approached and then rapidly declined when it was undermined. The water level in TP3 declined as the mine approached and continued to decline following undermining.

5 CONCLUSIONS

The impacts of longwall mining on ground water resources around a longwall face have been evaluated by use of a three-dimensional hydrmechanical coupled FE model. The evaluation is realized by determining the distribution of post-mining depressurization zones under undrained conditions.

Based on the characteristics of the distribution of post-mining overburden depressurization zones, it is concluded that changes in pressure head within the surface zone are quite different from those within the immediate zone. For the upper zone, the regions of depressurization are beyond the periphery of the mining panel with overpressured zones confined within the panel extent. For the lower zone, the regions of pressurization are outside the mining panel with depressurization within the panel extent. Therefore, the fluctuation of water levels in different wells will depend both on the depth and location of these wells relative to the mine layout and the proximity of mining. Behavior apparent from the distribution of volumetric strains (or changes in pore pressure) is consistent with field observations, typically made with monitoring wells of high system (volume) compressibility. The analysis assumes completely undrained conditions, but, despite potentially large changes in hydraulic conductivity that occur, post mining, define the appropriate sense of pore pressure change, and its distribution in space.

Although this hydromechanical coupled model is applied to a particular longwall mining site and conclusions drawn from this application have been used to explain observed results from other mining situations, cautions about the model limitations should be made when applying these conclusions. These limitations include the assumptions of the non-linear elastic deformation and the undrained conditions. When the long-term impacts of longwall mining on groundwater resources are of concern, post-mining hydraulic conductivity field should be incorporated into the groundwater flow model.

ACKNOWLEDGEMENTS

This work has been partially supported by the National Science Foundation under Grand No. CMS-9209059, and by the National Mined Land Reclamation Center under Grand No. CO388962. This support is gratefully acknowledged. The authors also thank two anonymous reviewers for providing critical comments and constructive suggestions in revising the manuscript.

REFERENCES

1. Neate, C. J. and Whittaker, B. J. Influence of proximity of longwall mining on strata permeability and ground water. In *Proceedings of US 22th Symposium on Rock Mechanics*, The University of Texas at Austin, 1979, pp. 217–224.
2. Booth, C. J. Hydrogeologic impacts of underground (longwall) mining in the Illinois basin. In *Proceedings of Third Workshop on Surface Subsidence due to Underground Mining*, ed. S.S. Peng, Department of Mining Engineering, West Virginia University, Morgantown, 1992, pp. 222–227.
3. Matetic, R. J., Trevits, M. A. and Swinehart, T. A case study of longwall mining and near-surface hydrological response. In *Proceedings of American Mining Congress-Coal Convention*, Pittsburgh, PA, 1991.
4. Matetic, R. J. and Trevits, M. Longwall mining and its effects on ground water quantity and quality at a mine site in the Northern Applachian coal field. In *Proceedings of FOCUS Conference on Eastern Regional Ground Water Issues*, 13–15 October 1992.
5. Matetic, R. J. An assessment of longwall mining-induced changes in the local ground water system. In *Proceedings of FOCUS Conference on Eastern Regional Ground Water Issues*, 27–29 September 1993.
6. Walker, J. S. *Case study of the effects of longwall mining induced subsidence on shallow ground water sources in the Northern Appalachian Coalfield*. RI9198 Bureau of Mines, United States Department of the Interior, 1988.
7. Hasenfus, G. J., Johnson, K. L. and Su, D. H. W. A hydromechanical study of overburden aquifer response to longwall mining. In *Proceedings of 7th International Conference on Ground Control in Mining*, ed., S.S. Peng, 1990, pp. 149–162.
8. Bai, M. and Elsworth, D. Transient poroelastic response of equivalent porous media over a mining panel. *Engineering Geology*, 1993, **35**, 49–64.
9. Bai, M. and Elsworth, D. Dual-porosity poroelastic approach to behavior of porous media over a mining panel. *Trans. Inst. Min. and Min.*, 1993, **102**, A114–A124.
10. Elsworth, D., Liu, J. and Ouyang, Z. Some approaches determine the potential influence of longwall mining on ground water resources. In *Proceedings of International Land Reclamation and Mine Drainage Conference and 3rd International Conference on the Abatement of Acidic Drainage*, vol IV, Pittsburgh, PA, USA, 1994, pp. 172–179.
11. Liu, J. *Topographic influence of longwall mining on water supplies*. Master's Thesis, Department of Mineral Engineering, The Pennsylvania State University, University Park, PA, 1994.
12. National Coal Board. *Subsidence Engineer's Handbook*, United Kingdom, 1966.
13. Biot, M. A. General theory of three-dimensional consolidation. *J. Appl. Phys.*, 1941, **12**, 155–164.
14. Detournay, E. and Cheng, H. Constitutive equations-theoretical background. In *Poroelasticity in Rock Mechanics*, ed., E. Detourney, University of Wisconsin-Madison, 26–27 June 1993, pp. 1–28.
15. Detournay, E. and Cheng, H.-D. Fundamentals of poroelasticity In J.A. Hudson, *Comprehensive Rock Engineering*, vol. 2, Pergamon Press, Oxford, 1993, pp. 113–172.
16. Matetic, R. J., Liu, J. and Elsworth, D. Modeling the effects of longwall mining on the ground water system. In

Proceedings of the 35th US Symposium on Rock Mechanics, eds., J.J.K. Daemen and R.A. Schiltz, 1995, pp. 639–644.
17. Elsworth, D. and Liu, J. Topographic influence of longwall mining on ground water supplies. *Ground Water*, 1994, Autumn.
18. Liu, J. *Numerical studies toward a determination of the impact of longwall mining on ground water resources*. Ph.D. Thesis, The Pennsylvania State University, University Park PA 16802, 1996.
19. Liu, J., Elsworth, D. and Matetic, R. J. Evaluation of post-mining ground water regime. *Hydrological Processes*, 1997, **11**, 1945–1961.
20. Bai, M. and Elsworth, D. Modeling of subsidence and stress-dependent hydraulic conductivity for intact rock and fractured porous media. *Rock Mech. and Rock Engng.*, 1994, **27**(4), 209–234.
21. Van Roosendaal, D. J. *et al.* Overburden deformation and hydrological changes due to longwall mine subsidence in Illinois. In *Proceedings of 3rd Conference on Ground Control Problems in the Illinois Coal Basin*, ed., Y.P. Chung, Mt. Vernon IL, 1990 pp. 73–82.